Challenge Journal of Structural Mechanics

Research Article

Earthquake performance of collapsed school building under Van-Tabanli (Mw=7.2) earthquake

Cumhur Cosgun [a,*], Atakan Mangir [b]

[a] *College of Information Technology and Engineering, Marshall University, Huntington, WV 25755, USA*
[b] *Institute of Graduate Studies in Science and Engineering, İstanbul University, 34320 İstanbul, Turkey*

ABSTRACT

A majority of the present building stock of Turkey is under seismic risk. It is believed that a significant proportion of the existing structures will either collapse or will get heavily damaged during a possible strong earthquake. With this respect, as an initial stage in the betterment of the structurally deficient building stock, assessment of existing buildings is of vital importance. From this viewpoint, in this study, earthquake performance of a collapsed school building was investigated through numerical performance analysis based on codified rules. At the end of 2011, numerous ground motions of various intensities have been registered in city of Van in eastern Turkey starting from 23 October 2011. Two major earthquakes were experienced at the Tabanli and Edremit district of Van. The moment magnitudes of these earthquakes were announced as 7.2 and 5.6, respectively. The investigated school building in this study was located in the city of Van and collapsed after first major earthquake (Mw=7.2). Structural details of the load-bearing members of the investigated building including as-built drawings and specified material properties were obtained. Based on obtained data, a numerical model was created to simulate the behavior of the building under code specified earthquake effects. Earthquake performance assessment of the structure was carried based on the recommendations given in the related chapter of the Turkish Seismic Code. Pushover analyses were performed and expected member by member damage levels and overall structural damage were determined in accordance with Turkish Seismic Code. The results are discussed to enlighten the actual cause of the collapse.

ARTICLE INFO

Article history:
Received 5 September 2018
Revised 12 October 2018
Accepted 30 October 2018

Keywords:
Collapsed school building
Earthquake performance
Nonlinear static analysis
Damage evaluation

1. Introduction

A majority of the present building stock of Turkey is under seismic risk. With this respect, it is believed that a significant proportion of the existing structures will either collapse or will get heavily damaged during a possible strong earthquake. This is well supported by the consequences of the previous earthquakes that occurred in the region (1992 Erzincan, 1995 Dinar, 1998 Adana-Ceyhan, 1999 Kocaeli and Düzce).

At the end of 2011, numerous ground motions of various intensities have been registered in city of Van in Turkey starting from 23 October 2011. Two major earthquakes were experienced at the Tabanli and Edremit district of Van. The moment magnitudes of these earthquakes were announced as 7.2 and 5.6, respectively, by United States Geological Survey (USGS). In these seismic events 604 people lost their life and 1000 buildings were either heavily damaged or collapsed. More than 600,000 people were reported to have been affected by the earthquakes in that period (Cosgun et al., 2013).

A major part of earthquake prone areas in the world hold sub-standard building stocks. Buildings constructed with poor reinforcement details, low strength concrete (under 10 MPa) and reinforcing bars with plain surfaces generally suffer from earthquakes due to low

* *Corresponding author*. Tel.: +1-304-972-2699 ; Fax: +1-304-696-5454 ; E-mail address: cosgun@marshall.edu (C. Cosgun)
ISSN: 2149-8024 / DOI: https://doi.org/10.20528/cjsmec.2018.04.004

deformation and lateral load-carrying capacity (Ilki et al., 2009; Bedirhanoglu et al., 2010; Cosgun et al., 2013; Turk et al., 2013). These buildings are urgently needed to be either reconstructed or strengthened to reduce human losses in possible future strong seismic events. During the structural renewing of sub-standard buildings, efficient numerical simulation and assessment methodologies will considerably contribute to the reduction of damages in future earthquakes. On the other hand, the real cases experienced in past earthquakes are quite important to evaluate the efficiency of these numerical simulation approaches and code-specified member performance criteria. Isik and Kutanis (2015) have conducted performance-based assessment for existing residential buildings to investigate the seismicity of the region, recently.

During the aforementioned seismic events in the city of Van, unfortunately, some government buildings were heavily damaged or collapsed. One of these collapsed buildings is the Gedikbulak school building. This building is the only school building that collapsed in the region. Fortunately, at the time of collapse there were no students or staff nor any visitors inside the building. In this study, this building was chosen to investigate the earthquake performance by using numerical simulation based on present seismic code requirements for the assessment of existing RC buildings. Nonlinear pushover analyses were carried out for the building for both orthogonal lateral directions. During the nonlinear seismic performance assessment analyses, the design blue prints were taken into consideration. Therefore, the main purpose of the study is to check the suitability or safety of the design approach followed during the construction of the school building. Finally, seismic performance levels defined in the current code of practice were used to compare with strength and drift estimations from the numerical simulations. Inel and Meral (2016)'s study also shows the approach of Turkish Seismic Code (TSC, 2007) on the seismic performance of RC buildings subjected to past earthquakes in Turkey and encountered damage types from the effects of previous earthquakes.

2. Strong Ground Motion Records and Spectral Characteristics

Local coordinates of the Mw=7.2 Tabanli and Mw=5.6 Edremit earthquakes are reported as 38.689N–43.465E and 38.447N–43.263E, respectively (AFAD). While the maximum PGA values recorded during the Tabanli earthquake at the Muradiye station for NS, EW, and Vertical directions are 0.182g, 0.173g, and 0.081g, respectively, the maximum PGA values recorded during the Edremit earthquake at the Van Merkez station in the NS, EW, and Vertical directions, are 0.151g, 0.251g, and 0.153g, respectively. For the Tabanli earthquake, the processed time histories yield peak ground velocities of 27.3 cm/s, 14.8 cm/s, and 5.9 cm/s for the NS, EW, and Vertical components, respectively; whereas the maximum peak ground displacement is obtained as 5.5 cm for the NS component (Tapan et al., 2013). For the Edremit earthquake, peak ground velocities of 17.3 cm/s, 32.1 cm/s, and 6.3 cm/s are obtained for the NS, EW, and Vertical components, respectively; whereas the maximum peak ground displacement is calculated as 6.8 cm for the EW component (Tapan et al., 2013). The 5% damped acceleration response spectra obtained from the records of the Tabanli and Edremit earthquakes are compared with the 2007 Turkish Seismic Code (TSC, 2007) spectrum in Fig. 1, defined for seismic zone 1 (PGA=0.4g) for Van and for all soil classes, where Z1 represents the most stiff soil condition and Z4 the softest. In the TSC (2007), the shortest period range for a maximum spectral amplification value of 2.5 is defined between period values of TA=0.10s and TB=0.30s for soil class Z1, and the longest period range is defined between period values of TA=0.20s and TB=0.90s for soil class Z4. As seen in Fig. 1, none of the records exceed the design spectra.

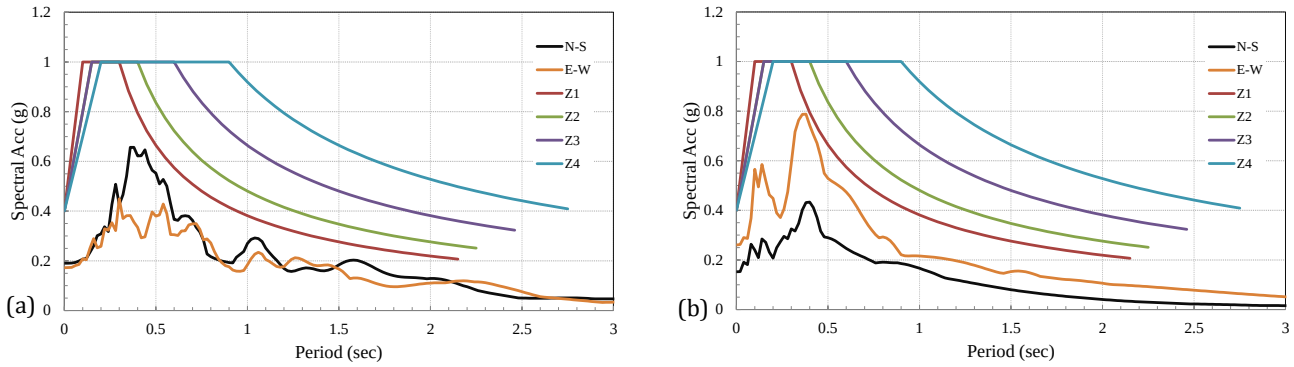

Fig. 1. Comparison of (a) first (Muradiye station) and (b) second earthquake (Van Merkez station) response spectrum with TSC (2007) design spectrum.

3. Outline of Investigated School Building

School buildings in the city center and districts are generally low-rise reinforced concrete structures with shear walls. While, owing to presence of sufficient amount of shear walls in two main orthogonal directions and the regular structural systems, most of these school buildings have performed well, without experiencing considerable damage, few school buildings have experienced widespread damage in partition walls. Considering the possibility of school buildings to be used as shelters after earthquakes, this type of non-structural damage

should also be avoided through proper construction of the partition walls. Few schools, particularly relatively older ones without shear walls, experienced slight to moderate structural damage as well. However, among all the above-mentioned school buildings, there was one school building (Gedikbulak school building) that totally collapsed.

The structure is a 3-storey building which was constructed in 1988 having dimensions 14.4 by 21.6 m in plan. It has four spans in both E-W (X) and N-S (Y) directions. The story height of all stories is 3.2 m. The typical architectural and structural floor plans of the building is shown in Fig. 2. View of the collapsed school building is also given in Fig. 3.

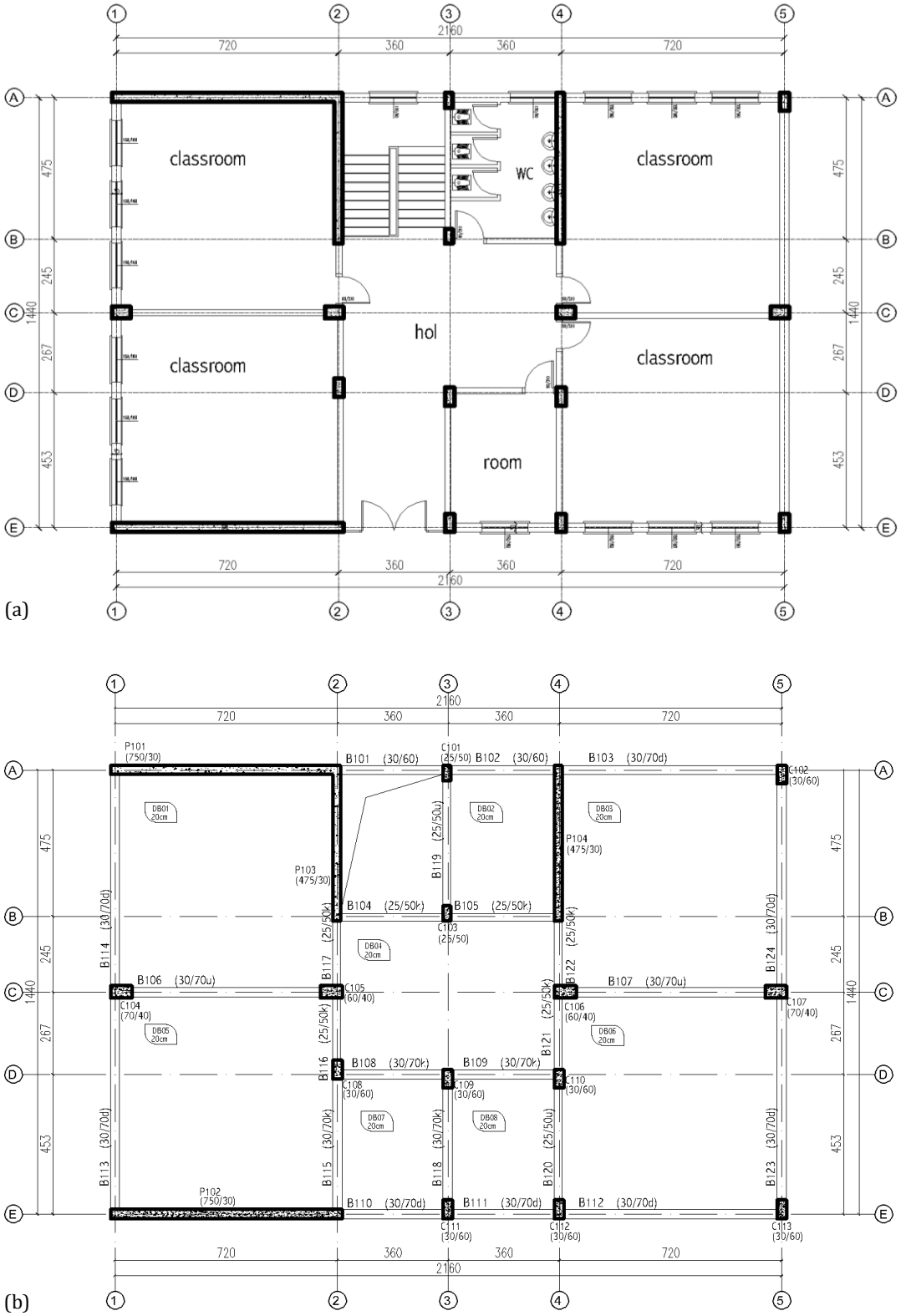

Fig. 2. (a) Architectural and (b) Structural floor plans of the collapsed school building.

Fig. 3. View of the collapsed school building.

Information regarding the structural system plan and geometric details of the structural members were obtained by in-situ investigation. As-built drawings of the building were also available and these were used to cross-check the in-situ investigation findings. The cross-section details of the building columns and beams are shown in Figs. 4 and 5. The building was constructed with two-way reinforced concrete slabs having thickness of 200 mm. Main differences between the section types are the dimensions and longitudinal reinforcement configuration. The building has 2 types of shear walls with two different cross-section geometries as rectangular and L-shaped. Both types of shear walls include ϕ18 bars as longitudinal reinforcement on first floor. On upper floors, shear walls have same dimensions but with ϕ14 bars. Layout of the geometric cross-sectional details of structural members is given on the floor plan in Fig. 2. Plain bar type reinforcements were used for all the structural members of the building

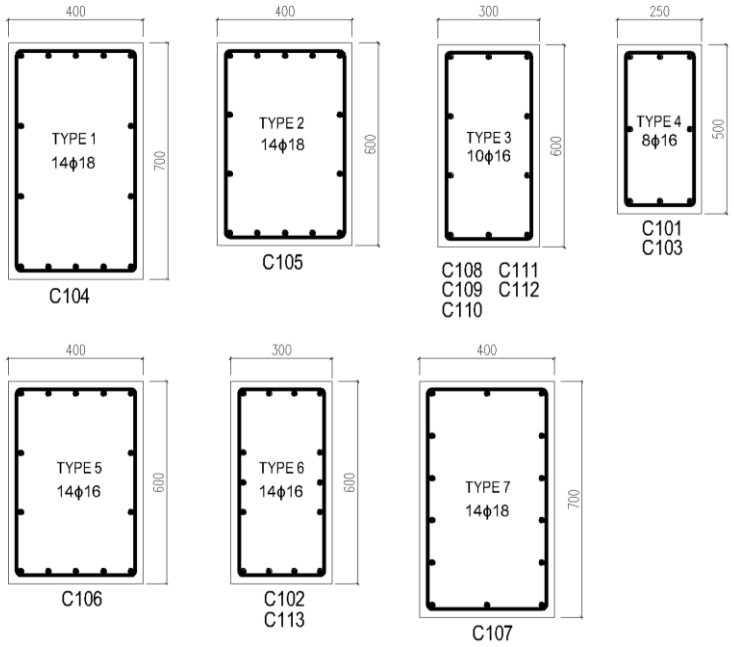

Fig. 4. The geometry and structural details of column cross sections.

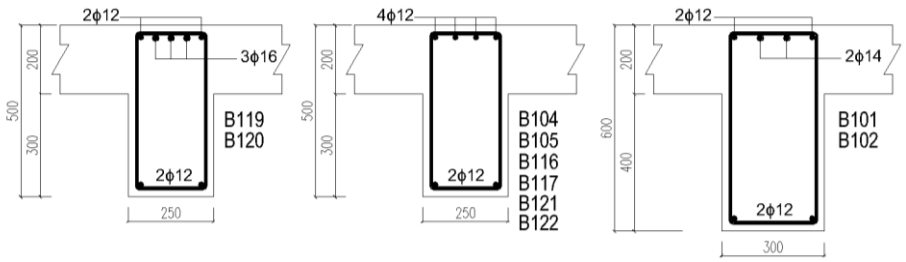

Fig. 5. The geometry and structural details of beam cross sections.

4. Damage Outline and Construction Errors

Damage outline of the collapsed building is presented under this chapter. Fig. 6 presents post-earthquake photographs of this collapsed building. Also, in Fig. 7, a close-up photograph of one of the failed shear walls in the building at first floor level is shown. It is observed that the shear walls were lacking all necessary conditions that are dictated by the related Turkish Seismic Design Code (TSC, 2007). These include inadequate lap splices, poor reinforcement details, insufficient concrete strength and the use of plain reinforcement bars. Some of these deficiencies can also be observed from the buildings in Kütahya region of Turkey after 2011 Simav earthquake (Yön et al., 2013).

Fig. 6. Photos of the collapsed school building.

As will be demonstrated in the following pages, the nonlinear static analysis of the building carried out by assuming the project member sizes and reinforcement details has revealed that the structural system appears to be adequate, in terms of stiffness and strength, to withstand these moderate-level earthquakes without total collapse. However, the deficiencies in reinforcement detailing such as insufficient anchorage of the beam longitudinal bars into the shear walls (see Fig. 6), low stirrup spacing and the lack of hooks of lateral reinforcement, and inadequate lap splices of the longitudinal bars of the shear walls seem to have impaired the efficiency of the shear walls, remarkably (see Fig. 7). The collapse mechanisms encountered in this observation can be compared and discussed with the study on the seismic behavior of a reinforced concrete building collapsed during the 2009 L'Aquila earthquake (Palermo et al. 2014). In 2009 L'Aquila earthquake, some of the buildings were totally collapsed building revealed that most of the columns at the ground story level failed in shear with some evident buckling of the longitudinal bars (no transverse reinforcement in the joint region).

5. Nonlinear Static Analysis

Seismic assessment of existing structures are complicated work which generally requires more sophisticated analyses than performing a new design (Ni, 2014). Carvalho et al. (2013) have compared different modelling approaches for nonlinear static and dynamic analyses of reinforced concrete buildings. In this study, three dimensional analyses were conducted using the structural analysis program SAP2000 (CSI, 2016) for static and dynamic analysis of structure. The cross-section properties like moment-curvature capacities for beam ends and normal force – moment (P-M) interaction curves for shear wall ends were calculated by using the XTRACT software (IMBSEN software systems, 2004). A description of the modelling details is provided as follows. A three-dimensional model of the structure which is shown in Fig. 8 was created with the software to carry out the nonlinear static analysis. Beam and column elements were modelled as nonlinear frame elements with lumped plasticity by defining plastic hinges at both ends of the beams and both ends of the columns. Theoretical

zero distances were assumed for the plastic hinge locations. Shear walls are modelled like frame members by defining the geometric properties of shear walls. The user defined flexural hinge properties were determined by the moment–curvature and P-M interaction analyses of each structural element by means of the section analysis software. Moment – rotation diagrams of beams and P-M interaction diagrams of shear-walls are gathered from the analysis by XTRACT software. And for columns, SAP2000's sectional plastic analysis configuration is used.

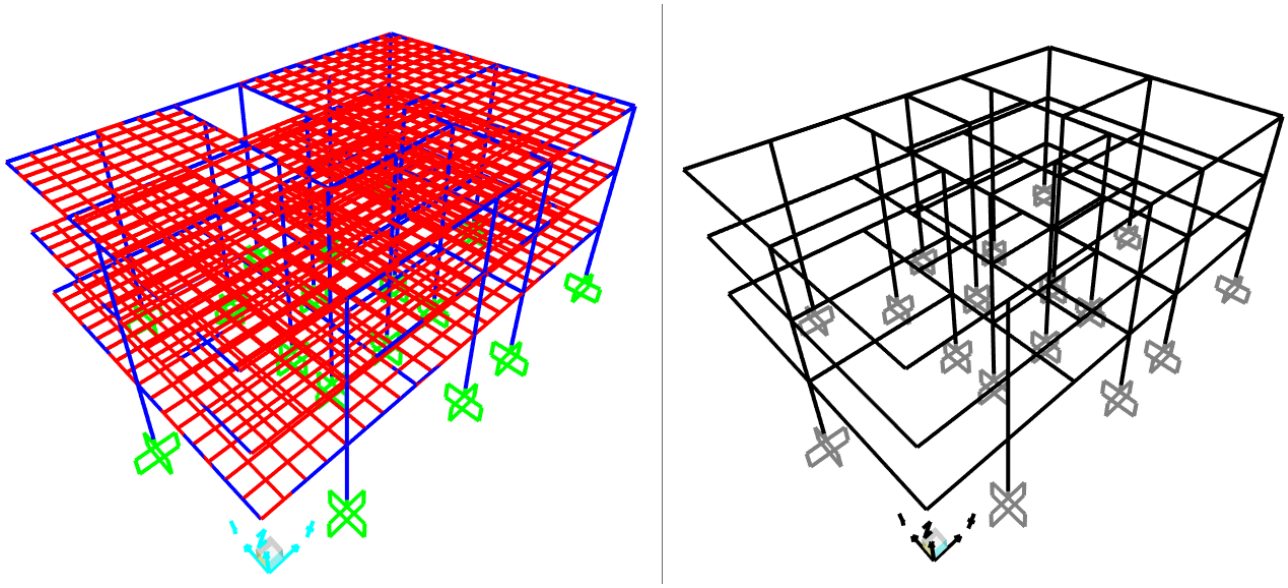

Fig. 8. 3D model of the structure.

The nonlinear behavior of columns and beams are taken into consideration through the defined plastic hinges at the critical locations where moments are maximum. The inelastic moment-rotation relationships of columns and beams are obtained through fiber analysis using build-in SAP2000 tools and XTRACT software, respectively. The reason of using SAP2000 built-in tool for determination of moment-rotation relationship of columns is the variation of axial loads on the columns, which was not possible to take into consideration for moment-rotation relationships to be obtained using XTRACT software, which takes into account a constant axial load for the member. On the other hand, use of XTRACT software for the moment-rotation relationships of the beams does not pose any problem since axial loads on the beams are marginally small. The moment-rotation relationships for beams are obtained through XTRACT software rather than SAP2000 due to more practical data input interface of XTRACT. It should also be noted that after determination of P-M relationship for columns, SAP2000 assumes a bilinear moment-rotation relationship with a horizontal branch after yielding. The material models for the unconfined concrete (f_c=10 MPa), confined concrete and the typical steel stress–strain model with strain hardening for steel (f_y=220 MPa) used in the moment–curvature analyses is given in Figs. 9 and 10. These material models are specified in related TSC (2007) code which states to use Mander and Priestley's material model for confined concrete (Mander et al., 1988). Live load on the structure is defined as 3.5 kN/m^2 and 2.0 kN/m^2 floor covering load is defined. Dead load is automatically calculated by the software.

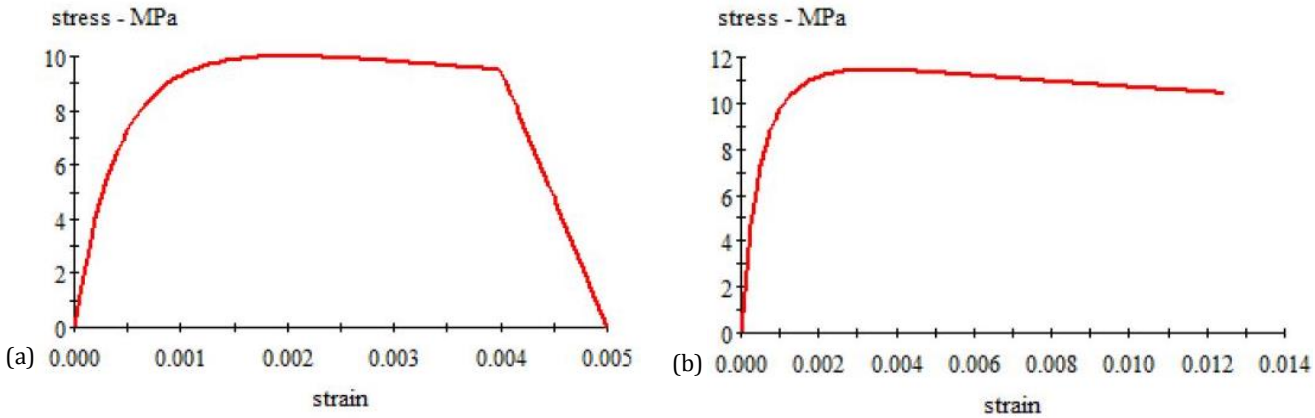

Fig. 9. (a) Unconfined and (b) Confined concrete material models used in the analysis for C10.

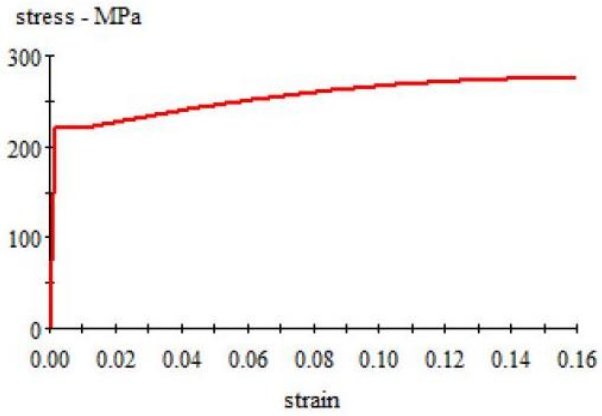

Fig. 10. Stress–strain model with strain hardening for reinforcing steel (f_y=220 MPa).

The cracked section stiffness for RC beams was assumed as 0.4 times of EI (flexural rigidity of cross section) according to TSC (2007). As stated in TSC (2007), live load participation for school buildings is given as "0.6" and the cracked section stiffness for RC columns should be calculated after analysis of structure under "Dead Load + (live load participation factor) x (Live load)" combination. Cracked section stiffness values for RC columns are dependent on the axial load of those members under the combination mentioned above. Cracked section stiffness of each column and shear wall is calculated and defined in the software. Related rule in TSC (2007) is given below:

If $N_D / (A_c f_{cm}) \leq 0.10$ then $(EI)_c = 0.40\,(EI)$

If $N_D / (A_c f_{cm}) \geq 0.40$ then $(EI)_c = 0.80\,(EI)$

If $0.10 < N_D / (A_c f_{cm}) < 0.40$ then Interpolation for $(EI)_c$

where: N_D = axial force on member; A_c = cross sectional area of member; f_{cm} = compressive strength of concrete; EI = flexural rigidity of cross section; $(EI)_c$ = the cracked section stiffness.

In the nonlinear static (pushover) analysis, the behavior of the structure is characterized by the capacity curve that represents the relationship between the base shear force and top displacement. This is a very convenient representation in practice, and can easily be visualized by structural engineers. It is recognized that the structure's roof displacement is used for the capacity curve because it is widely accepted in practice. The structure is investigated in both orthogonal horizontal directions. Analysis case for x direction was named PushX while PushY was used for y direction. As analysis results, "pushover curves of both cases are converted to modal capacity diagrams and superposed with design earthquake spectrum with bilinear curves. Deflection demand curves for both cases are given in Figs. 11 and 12.

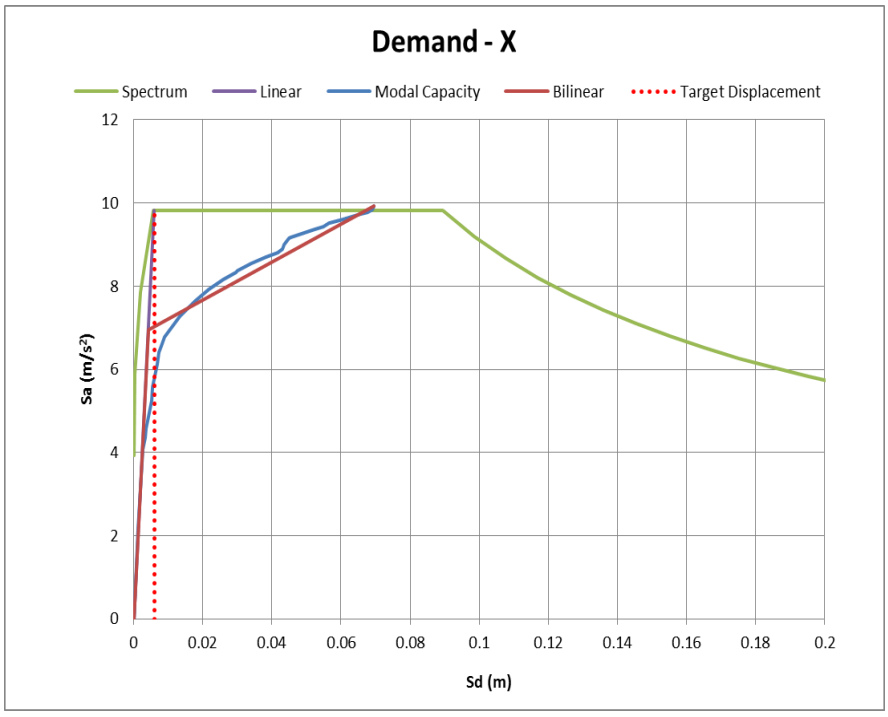

Fig. 11. Deflection demand for PushX case.

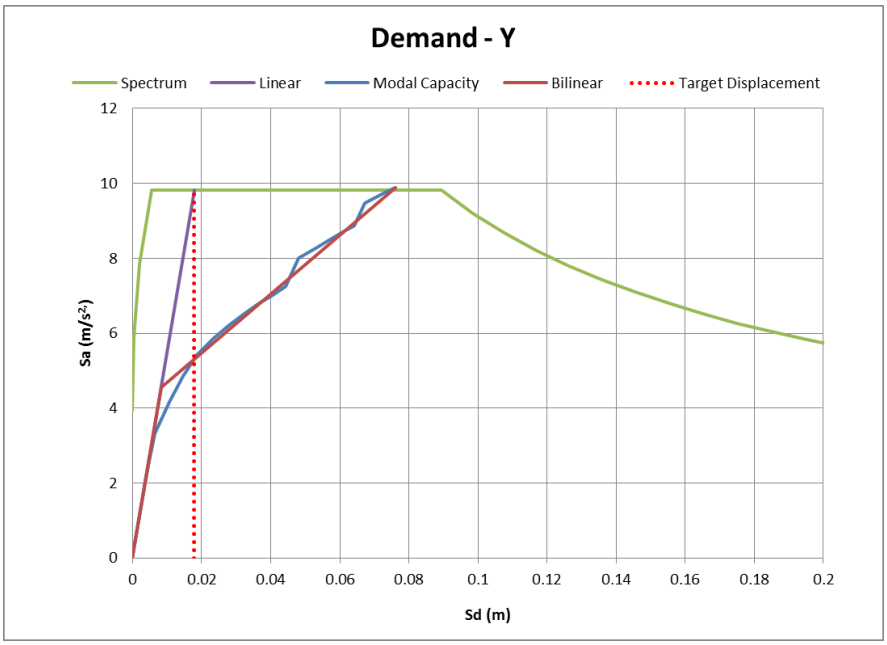

Fig. 12. Deflection demand for PushY case.

TSC (2007) specifies that the target displacement (S_{di}) gathered from the graph should be increased by multiplying the S_{di} value with modal participation factor (Γ_{i1}) and mode shape roof displacement (Φ_{iN1}) of related mode. The target roof displacements calculated for PushX case was calculated as 0.014 m and it was calculated as 0.040 m for PushY. The structure is re-pushed until target displacement values are reached and plastic hinge mechanisms in last step of both directions (PushX and PushY cases) are investigated. Plastic hinge formation pattern for the initial hinges and the hinges at target displacement state (PushX and PushY cases) are shown in Fig. 13.

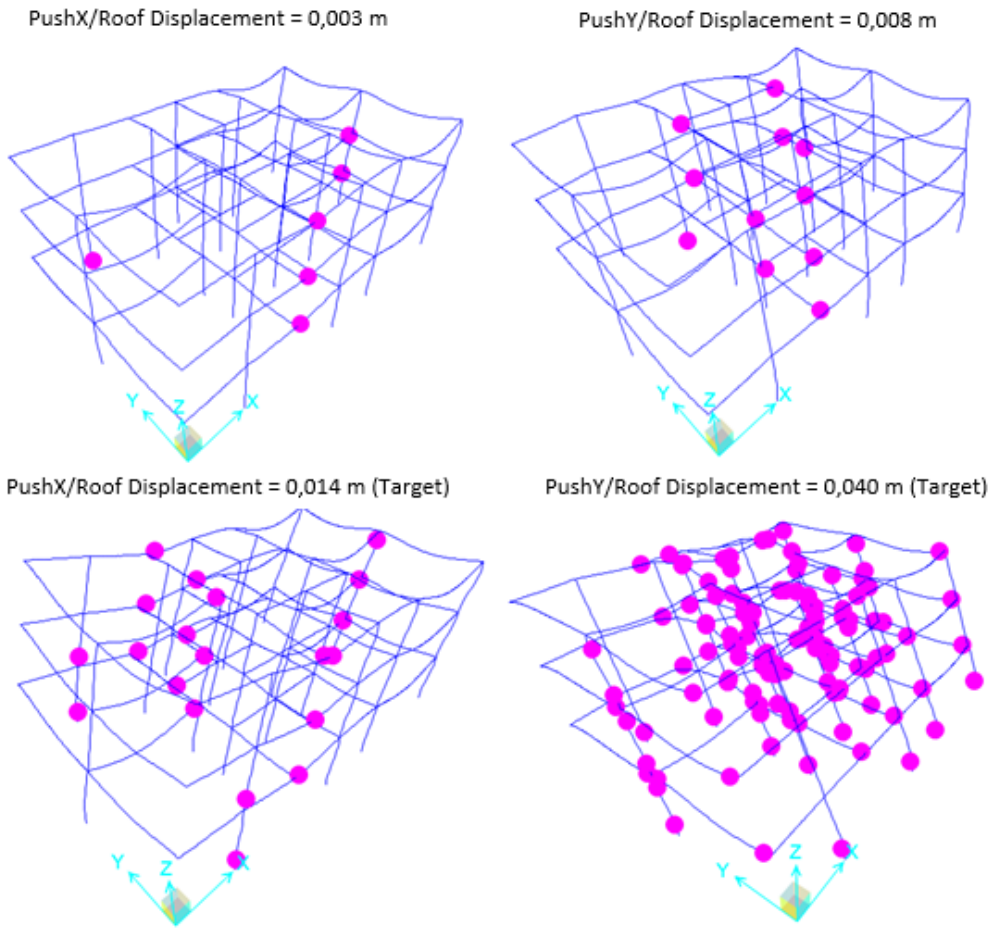

Fig. 13. Plastic hinge formation pattern for PushX and PushY cases.

As seen in these figures, according to design approach followed, plastic hinges occur on columns and beams. Therefore, it is obvious that the current capacity design principles were not followed properly during the design phase leading to weak columns and strong beams. Nevertheless, at target drift, the building is still in life safety performance level. Plastic hinge formation mechanisms were obtained at displacement points corresponding to the global yielding and ultimate displacements. The global yielding point corresponds to the displacement along the capacity curve in which the system starts to soften. No shear failure of structural members was detected in both cases. This was primarily due to the assumed low compressive strength of concrete and weak joint detailing. Thus, the overall behavior was dominated by the flexure and joint shear.

After the pushover analysis, plastic rotation of each hinge mechanism is checked for the rules given in TSC (2007). In the current Turkish Seismic Code, three different damage limits are defined in terms of plastic strain of concrete and steel for the evaluation of structural performance. Details of these damage limits are given in Table 1.

The code describes four different performance levels: Light Damage, Moderate Damage, Heavy Damage and Collapse, as shown in Fig. 14.

Table 1. Section damage limits given in TSC (2007).

Section Damage Limit	Unconfined Concrete		Confined Concrete	
	Strain of Concrete (ε_c)	Strain of Steel (ε_s)	Strain of Concrete (ε_c)	Strain of Steel (ε_s)
Minimum Damage Limit (MN)	0.0035	0.01	0.0035	0.01
Safety Limit (SL)	0.0035	0.04	0.0135	0.04
Failure Limit (FL)	0.0035	0.06	0.0180	0.06

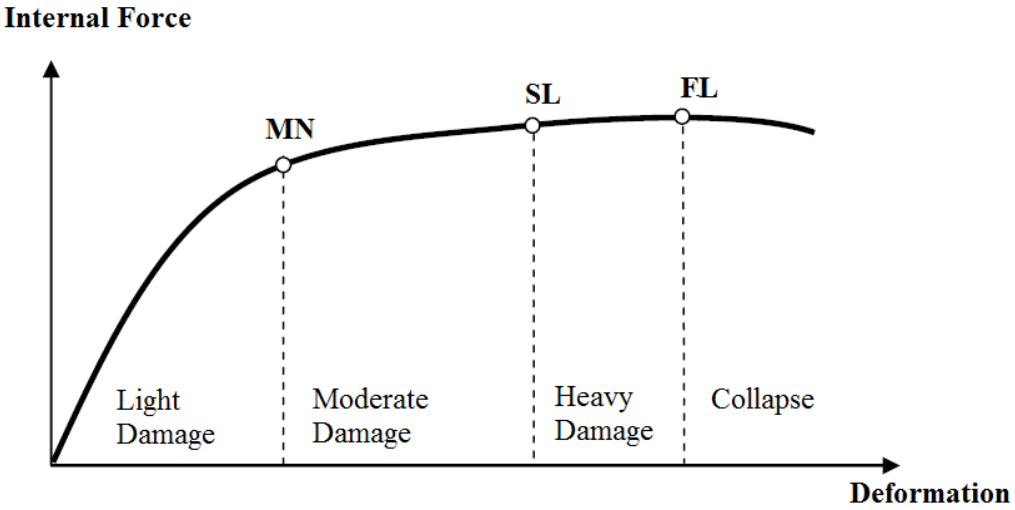

Fig. 14. Performance levels for structural members given in TSC (2007).

According to TSC (2007), plastic curvature demand of a structural member is found as;

$$\phi_p = 9\,\theta_p / L_p\,, \quad (1)$$

where; L_p is the plastic hinge length of member which is depth/2, θ_p values are the plastic rotation of hinges in last step of pushover analysis.

Total curvature demand is calculated by Eq. (2) as;

$$\phi_t = \phi_p + \phi_y\,, \quad (2)$$

where; ϕ_y is the curvature at first yield, gathered from cross-section analysis in XTRACT program for each section.

After calculating the total curvature demand ϕ_t, the compressive strain of concrete (ε_c) and tensile strain of reinforcement bars (ε_s) at that total curvature is found by sectional analysis in XTRACT software.

Storey drift ratio checks for both cases were made. A story drift ratio of 0.02 is given for Life Safety limit in TSC (2007). Storey drift ratio checks are given in Table 2 for both PushX and PushY cases. It is observed that story drift ratios calculated for both directions meet the Life Safety performance limits.

Table 2. Storey drift ratio checks for PushX and PushY cases.

Storey	h (m)	Push X	Storey Drift Ratio		Life Safety Limit	Control
		δi_{max} (m)	$\delta i / h$			
1	3.2	0.0039	0.0012	<	0.02	OK
2	3.2	0.0049	0.0015	<	0.02	OK
3	3.2	0.0050	0.0016	<	0.02	OK
Storey	h (m)	Push Y	Storey Drift Ratio		Life Safety Limit	Control
		δi_{max} (m)	$\delta i / h$			
1	3.2	0.0116	0.0036	<	0.02	OK
2	3.2	0.0136	0.0043	<	0.02	OK
3	3.2	0.0136	0.0043	<	0.02	OK

Shear Capacity Control of structural members are carried under the maximum shear demand (V_{max}) gathered from PushX and PushY cases for different sections. According to TSC (2007), following shear calculations are used for shear failure assessment.

Concrete's contribution to section's shear strength is calculated with Eq. (3) as;

$$V_c = 0.8 \cdot 0.65 \cdot f_{ctm} \cdot b_w \cdot d(1 + 0.07 \cdot N/A_c)\,, \qquad (3)$$

where; f_{ctm} = tensile strength of concrete = $0.35\sqrt{f_{cm}}$; b_w = width of section; d = effective depth of tensile reinforcement; N = axial force on member; A_c = area of section.

Steel reinforcement bars' (stirrups) contribution to section's shear strength is calculated with Eq. (4) as;

$$V_s = A_s \cdot f_{ys} \cdot (d/s)\,, \qquad (4)$$

where; f_{ys} = yield strength of stirrups; A_s = Total area of stirrups; s = spacing of stirrups.

TSC (2007) states that if total sectional shear strength of member ($V_r = V_c + V_s$) is greater than maximum shear demand (V_{max}) under the last step of Pushover analysis, the section is safe against shear failure. In Table 3, shear capacity control of different cross-sections is presented.

Table 3. Shear capacity control of members.

Structural Member Type	V_c (kN)	V_s (kN)	V_r (kN)	V_{max} (kN)		Control
			($V_c + V_s$)	PushX	PushY	
25/50 Beams	66.96	40.83	107.79	41.14	86.64	OK
30/60 Beams	97.84	49.72	147.56	28.99	38.97	OK
30/70 Beams	114.98	58.43	173.41	130.99	129.17	OK
Type 1 Columns	176.99	72.93	249.92	86.52	137.82	OK
Type 2 Columns	132.14	61.93	194.07	107.36	92.87	OK
Type 3 Columns	118.89	62.04	180.93	31.50	129.58	OK
Type 4 Columns	87.18	51.04	138.22	16.28	64.68	OK
Type 5 Columns	133.80	62.04	195.84	61.87	79.68	OK
Type 6 Columns	111.54	62.04	173.58	45.66	104.51	OK
Type 7 Columns	186.71	72.93	259.64	161.95	139.66	OK

Maximum shear demand (V_{max}) values are obtained for each cross-section type among all structural members. In Table 6, shear capacity control of different cross-sections is presented. From the details in structural design project, beams and columns have single hoop stirrups (8 mm diameter) with 250 mm and 200 mm spacing as shear reinforcements, respectively. The results show that design shear forces do not exceed the calculated shear capacity for all the members considered.

The damage levels of beams under PushX and PushY cases are given in Tables 4 and 5. Abbreviations used are; "LD" for Light damage level, "MD" for Moderate damage level, "HD" for Heavy damage level and "CL" for collapse damage level.

It has been observed that for PushX case, all of the beams are in "Light Damage Level". In PushY case, B117, B217, B222 and B317 beams are in "Moderate Damage Level". Other beams are in "Light Damage Level".

Table 4. Performance level of beams under Push X case.

Member	B (m)	H (m)	Hinge No	L_p (m)	θ_p (rad)	ϕ_p	ϕ_y	ϕ_{tot}	ε_c	ε_s	Damage Level (Concrete)	Damage Level (Steel)	Result
B101	0.30	0.60	357H1	0.3	0.000678	0.002261	0.002250	0.004511	0.000248	0.002315	LD	LD	LD
			357H2	-	-	-	-	-	-	-	-	-	
B104	0.25	0.50	306H1	0.25	0.000182	0.000726	0.002727	0.003453	0.000207	0.001415	LD	LD	LD
			306H2	-	-	-	-	-	-	-	-	-	
B106	0.30	0.70	223H1	0.35	-	-	-	-	-	-	-	-	LD
			223H2	0.35	0.000883	0.002523	0.002185	0.004708	0.000567	0.002347	LD	LD	
B107	0.30	0.70	246H1	-	-	-	-	-	-	-	-	-	LD
			246H2	0.35	0.001368	0.003909	0.002185	0.006094	0.000902	0.005404	LD	LD	
B110	0.30	0.70	352H1	0.35	0.000837	0.002392	0.001859	0.004251	0.000330	0.005379	LD	LD	LD
			352H2	-	-	-	-	-	-	-	-	-	
B201	0.30	0.60	26H1	0.3	0.000857	0.002856	0.002250	0.005106	0.000248	0.002315	LD	LD	LD
			26H2	-	-	-	-	-	-	-	-	-	
B204	0.25	0.50	17H1	0.25	0.000208	0.000832	0.002727	0.003559	0.000207	0.001474	LD	LD	LD
			17H2	-	-	-	-	-	-	-	-	-	
B206	0.30	0.70	4H1	-	-	-	-	-	-	-	-	-	LD
			4H2	0.35	0.000808	0.002309	0.002185	0.004494	0.000567	0.002347	LD	LD	
B207	0.30	0.70	2H1	-	-	-	-	-	-	-	-	-	LD
			2H2	0.35	0.001232	0.003520	0.002185	0.005705	0.000567	0.002347	LD	LD	
B210	0.30	0.70	21H1	0.35	0.001057	0.003020	0.001859	0.004879	0.000330	0.005379	LD	LD	LD
			21H2	-	-	-	-	-	-	-	-	-	
B301	0.30	0.60	58H1	0.3	0.000665	0.002215	0.002250	0.004465	0.000248	0.002315	LD	LD	LD
			58H2	-	-	-	-	-	-	-	-	-	
B304	0.25	0.50	49H1	0.25	0.000078	0.000312	0.002727	0.003039	0.000189	0.001231	LD	LD	LD
			49H2	-	-	-	-	-	-	-	-	-	
B306	0.30	0.70	36H1	-	-	-	-	-	-	-	-	-	LD
			36H2	0.35	0.000042	0.000120	0.002185	0.002305	0.000380	0.001193	LD	LD	
B310	0.30	0.70	53H1	0.35	0.001052	0.003006	0.001859	0.004865	0.000330	0.005379	LD	LD	LD
			53H2	-	-	-	-	-	-	-	-	-	
B315	0.30	0.70	37H1	0.35	0.000107	0.000306	0.001895	0.002201	0.000181	0.001293	LD	LD	LD
			37H2	-	-	-	-	-	-	-	-	-	

In order to evaluate the seismic performance of columns, axial force-total curvature diagrams were established by indicating the previously mentioned damage limits. Seismic performance level of columns with axial force-total curvature diagrams is given in Fig. 15. From the pushover analysis, there is only one plastic hinge mechanism observed under PushX case at C307 column which is in Light Damage level. For PushY case, there are many plastic hinge mechanisms observed. Note that the figures represent results for seven different types of columns. The damage levels of columns under PushX and PushY cases are given in Table 6. As presented in Table 6, damage level for all the columns was determined as "Light Damage" level.

Table 5. Performance level of beams under Push Y case.

Member	B (m)	H (m)	Hinge No	L_p (m)	θ_p (rad)	ϕ_p	ϕ_y	ϕ_{tot}	ε_c	ε_s	Damage Level (Concrete)	Damage Level (Steel)	Result
B101	0.30	0.60	357H1	0.3	0.000248	0.000827	0.002250	0.003077	0.000205	0.001537	LD	LD	LD
			357H2	0.3	0.000066	0.000220	0.002424	0.002644	0.000284	0.001247	LD	LD	
B102	0.30	0.60	358H1	-	-	-	-	-	-	-	-	-	LD
			358H2	0.3	0.000164	0.000547	0.002250	0.002797	0.000195	0.001394	LD	LD	
B104	0.25	0.50	306H1	0.25	0.000904	0.003616	0.002992	0.006608	0.000437	0.002379	LD	LD	LD
			306H2	0.25	0.001407	0.005628	0.002727	0.008355	0.000365	0.005446	LD	LD	
B105	0.25	0.50	307H1	0.25	0.000220	0.000880	0.002727	0.003607	0.000214	0.001510	LD	LD	LD
			307H2	0.25	0.001050	0.004200	0.002992	0.007192	0.000437	0.002379	LD	LD	
B113	0.30	0.70	390H1	0.35	0.001875	0.005357	0.001859	0.007216	0.000330	0.005379	LD	LD	LD
			390H2	0.35	0.000850	0.002429	0.002458	0.004887	0.000860	0.002412	LD	LD	
B114	0.30	0.70	391H1	0.35	0.001311	0.003746	0.001859	0.005605	0.000330	0.005379	LD	LD	LD
			391H2	-	-	-	-	-	-	-	-	-	
B115	0.30	0.70	294H1	0.35	0.001937	0.005534	0.001895	0.007429	0.000400	0.005386	LD	LD	LD
			294H2	0.35	0.002883	0.008237	0.002099	0.010336	0.000831	0.006372	LD	LD	
B116	0.25	0.50	295H1	0.25	0.002145	0.008580	0.002727	0.011307	0.000365	0.005446	LD	LD	LD
			295H2	0.25	0.001062	0.004248	0.002992	0.007240	0.000437	0.002379	LD	LD	
B117	0.25	0.50	296H1	0.25	0.002835	0.011340	0.002727	0.014067	0.000444	0.008643	LD	LD	MD
			296H2	0.25	0.004958	0.019832	0.002992	0.022824	0.000991	0.011800	LD	MD	
B118	0.30	0.70	132H1	0.35	0.002461	0.007031	0.001895	0.008926	0.000400	0.005386	LD	LD	LD
			132H2	0.35	0.002320	0.006629	0.002099	0.008728	0.000831	0.006372	LD	LD	
B119	0.25	0.50	86H1	0.25	0.000306	0.001224	0.002860	0.004084	0.000462	0.005497	LD	LD	LD
			86H2	-	-	-	-	-	-	-	-	-	
B120	0.25	0.50	299H1	0.25	0.001055	0.004220	0.002860	0.007080	0.000462	0.005497	LD	LD	LD
			299H2	0.25	0.001833	0.007332	0.003320	0.010652	0.000930	0.005446	LD	LD	
B121	0.25	0.50	300H1	0.25	0.002075	0.008300	0.002727	0.011027	0.000365	0.005446	LD	LD	LD
			300H2	0.25	0.000783	0.003132	0.002992	0.006124	0.000437	0.002379	LD	LD	
B122	0.25	0.50	301H1	0.25	0.002403	0.009612	0.002727	0.012339	0.000365	0.005446	LD	LD	LD
			301H2	0.25	0.004586	0.018344	0.002992	0.021336	0.000810	0.008653	LD	LD	
B123	0.30	0.70	392H1	0.35	0.002224	0.006354	0.001859	0.008213	0.000330	0.005379	LD	LD	LD
			392H2	0.35	0.000586	0.001674	0.002458	0.004132	0.000765	0.002049	LD	LD	
B124	0.30	0.70	393H1	0.35	0.001519	0.004340	0.001859	0.006199	0.000330	0.005379	LD	LD	LD
			393H2	0.35	0.000501	0.001431	0.002458	0.003889	0.000728	0.001890	LD	LD	
B201	0.30	0.60	26H1	0.3	0.000331	0.001103	0.002250	0.003353	0.000215	0.001682	LD	LD	LD
			26H2	0.3	0.000191	0.000637	0.002424	0.003061	0.000299	0.001450	LD	LD	
B202	0.30	0.60	27H1	-	-	-	-	-	-	-	-	-	LD
			27H2	0.3	0.000300	0.001000	0.002250	0.003250	0.000202	0.001643	LD	LD	
B204	0.25	0.50	17H1	0.25	0.000691	0.002764	0.002992	0.005756	0.000422	0.002281	LD	LD	LD
			17H2	0.25	0.001230	0.004920	0.002727	0.007647	0.000365	0.005446	LD	LD	
B205	0.25	0.50	18H1	0.25	0.000121	0.000484	0.002727	0.003211	0.000197	0.001324	LD	LD	LD
			18H2	0.25	0.000887	0.003548	0.002992	0.006540	0.000437	0.002379	LD	LD	
B213	0.30	0.70	29H1	0.35	0.001673	0.004780	0.001859	0.006639	0.000330	0.005379	LD	LD	LD
			29H2	-	-	-	-	-	-	-	-	-	

Table 5 contd. Performance level of beams under Push Y case.

Member	B (m)	H (m)	Hinge No	L_p (m)	θ_p (rad)	ϕ_p	ϕ_y	ϕ_{tot}	ε_c	ε_s	Damage Level (Concrete)	Damage Level (Steel)	Result
B214	0.30	0.70	30H1	0.35	0.000085	0.000243	0.001859	0.002102	0.000157	0.001277	LD	LD	LD
			30H2	-	-	-	-	-	-	-	-	-	
B215	0.30	0.70	5H1	0.35	0.001878	0.005366	0.001895	0.007261	0.000400	0.005386	LD	LD	LD
			5H2	0.35	0.002291	0.006546	0.002099	0.008645	0.000831	0.006372	LD	LD	
B216	0.25	0.50	6H1	0.25	0.001841	0.007364	0.002727	0.010091	0.000365	0.005446	LD	LD	LD
			6H2	0.25	0.000691	0.002764	0.002992	0.005756	0.000422	0.002281	LD	LD	
B217	0.25	0.50	7H1	0.25	0.002268	0.009072	0.002727	0.011799	0.000365	0.005446	LD	LD	MD
			7H2	0.25	0.005033	0.020132	0.002992	0.023124	0.000991	0.011800	LD	MD	
B218	0.30	0.70	1H1	0.35	0.002259	0.006454	0.001895	0.008349	0.000400	0.005386	LD	LD	LD
			1H2	0.35	0.001707	0.004877	0.002099	0.006976	0.000831	0.006372	LD	LD	
B219	0.25	0.50	3H1	0.25	0.000138	0.000552	0.002860	0.003412	0.000319	0.002364	LD	LD	LD
			3H2	-	-	-	-	-	-	-	-	-	
B220	0.25	0.50	10H1	0.25	0.000804	0.003216	0.002860	0.006076	0.000462	0.005497	LD	LD	LD
			10H2	0.25	0.001268	0.005072	0.003320	0.008392	0.000930	0.005446	LD	LD	
B221	0.25	0.50	11H1	0.25	0.001911	0.007644	0.002727	0.010371	0.000365	0.005446	LD	LD	LD
			11H2	0.25	0.000648	0.002592	0.002992	0.005584	0.000422	0.002281	LD	LD	
B222	0.25	0.50	12H1	0.25	0.002098	0.008392	0.002727	0.011119	0.000365	0.005446	LD	LD	MD
			12H2	0.25	0.004629	0.018516	0.002992	0.021508	0.000991	0.011800	LD	MD	
B223	0.30	0.70	31H1	0.35	0.001752	0.005006	0.001859	0.006865	0.000330	0.005379	LD	LD	LD
			31H2	-	-	-	-	-	-	-	-	-	
B224	0.30	0.70	32H1	0.35	0.000602	0.001720	0.001859	0.003579	0.000215	0.002158	LD	LD	LD
			32H2	-	-	-	-	-	-	-	-	-	
B301	0.30	0.60	58H1	0.3	0.000201	0.000670	0.002250	0.002920	0.000197	0.001495	LD	LD	LD
			58H2	0.3	0.000068	0.000227	0.002424	0.002651	0.000284	0.001247	LD	LD	
B304	0.25	0.50	49H1	0.25	0.000529	0.002116	0.002992	0.005108	0.000413	0.002009	LD	LD	LD
			49H2	0.25	0.001223	0.004892	0.002727	0.007619	0.000365	0.005446	LD	LD	
B305	0.25	0.50	50H1	0.25	0.000106	0.000424	0.002727	0.003151	0.000186	0.001284	LD	LD	LD
			50H2	0.25	0.000945	0.003780	0.002992	0.006772	0.000437	0.002379	LD	LD	
B313	0.30	0.70	61H1	0.35	0.001075	0.003071	0.001859	0.004930	0.000330	0.005379	LD	LD	LD
			61H2	-	-	-	-	-	-	-	-	-	
B315	0.30	0.70	37H1	0.35	0.001432	0.004091	0.001895	0.005986	0.000400	0.005386	LD	LD	LD
			37H2	0.35	-	-	-	-	-	-	-	-	
B317	0.25	0.50	39H1	0.25	0.000839	0.003356	0.002727	0.006083	0.000243	0.002292	LD	LD	MD
			39H2	0.25	0.004504	0.018016	0.002992	0.021008	0.000991	0.011800	LD	MD	
B318	0.30	0.70	33H1	0.35	0.001037	0.002963	0.001895	0.004858	0.000400	0.005386	LD	LD	LD
			33H2	0.35	-	-	-	-	-	-	-	-	
B322	0.25	0.50	44H1	0.25	0.000867	0.003468	0.002727	0.006195	0.000243	0.002292	LD	LD	LD
			44H2	0.25	0.004188	0.016752	0.002992	0.019744	0.000810	0.008653	LD	LD	
B323	0.30	0.70	63H1	0.35	0.000792	0.002263	0.001859	0.004122	0.000330	0.005379	LD	LD	LD
			63H2	-	-	-	-	-	-	-	-	-	

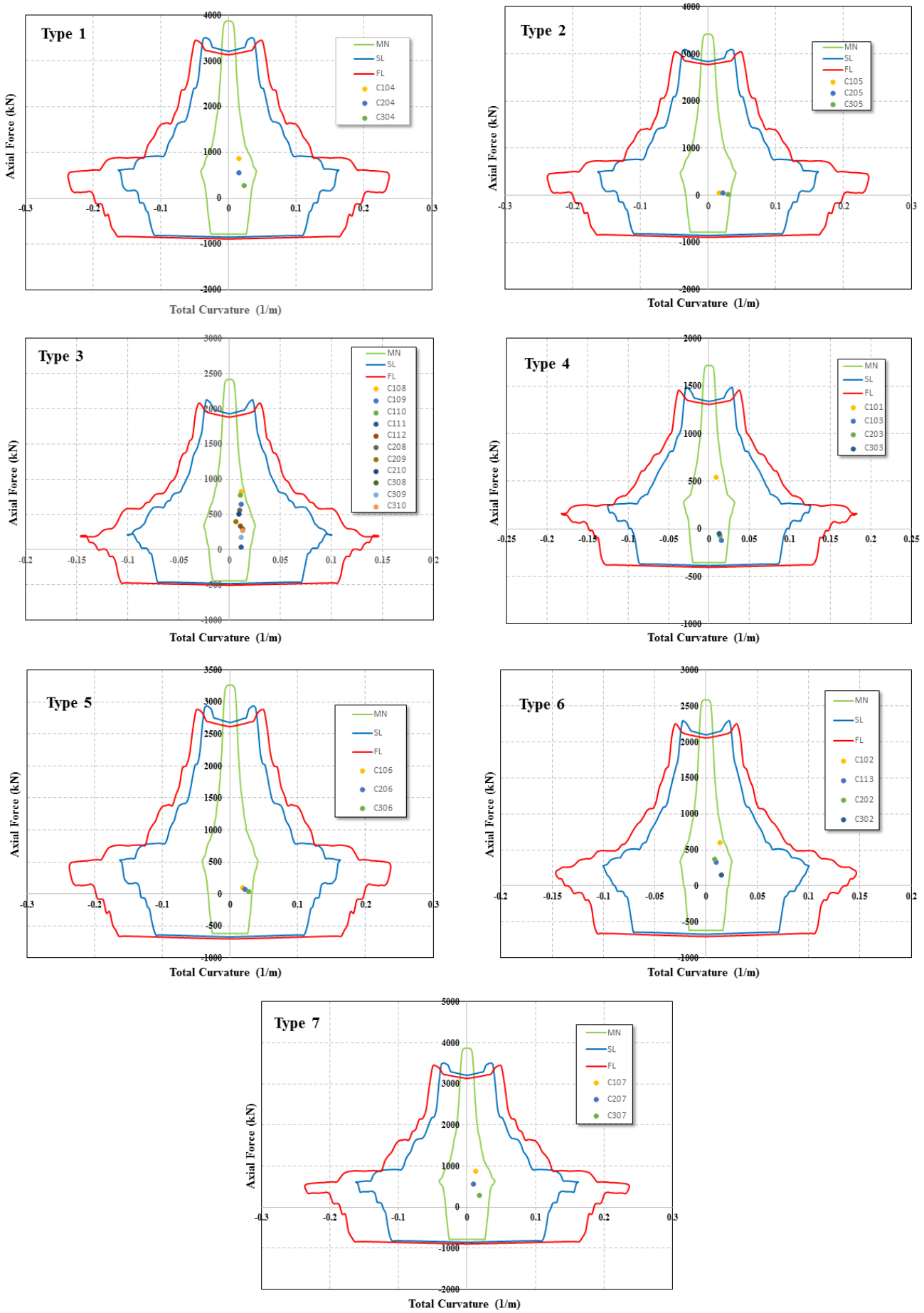

Fig. 15. Performance level evaluation of columns.

Table 6. Performance level of columns.

Member	P (kN)	B (m)	H (m)	Hinge No	L_p (m)	θ_p (rad)	ϕ_p	ϕ_y	ϕ_{tot}	Result
C101	538.93	0.25	0.50	270H1	0.25	0.001164	0.004656	0.004277	0.008933	LD
				270H2	-	-	-	-	-	
C102	595.59	0.30	0.60	274H1	0.15	0.000736	0.004907	0.008646	0.013553	LD
				274H2	-	-	-	-	-	
C103	117.48 (T)	0.25	0.50	266H1	0.25	0.003177	0.012708	0.002762	0.015470	LD
				266H2	0.25	0.002377	0.009508	0.002762	0.012270	
C104	860.18	0.70	0.40	250H1	0.20	0.001934	0.009670	0.006110	0.015780	LD
				250H2	0.20	0.000015	0.000075	0.006110	0.006185	
C105	55.93	0.60	0.40	254H1	0.20	0.002467	0.012335	0.004374	0.016709	LD
				254H2	0.20	0.002267	0.011335	0.004374	0.015709	
C106	93.52	0.60	0.40	258H1	0.20	0.002563	0.012815	0.004337	0.017152	LD
				258H2	0.20	0.002802	0.014010	0.004337	0.018347	
C107	877.94	0.70	0.40	262H1	0.20	0.001294	0.006470	0.006159	0.012629	LD
				262H2	-	-	-	-	-	
C108	825.90	0.30	0.60	237H1	0.30	0.002397	0.007990	0.003323	0.011313	LD
				237H2	-	-	-	-	-	
C109	641.76	0.30	0.60	241H1	0.30	0.002207	0.007357	0.004013	0.011370	LD
				241H2	-	-	-	-	-	
C110	770.62	0.30	0.60	245H1	0.30	0.002224	0.007413	0.003491	0.010904	LD
				245H2	-	-	-	-	-	
C111	39.15	0.30	0.60	225H1	0.30	0.002553	0.008510	0.002679	0.011189	LD
				225H2	-	-	-	-	-	
C112	334.01	0.30	0.60	229H1	0.15	0.000504	0.003360	0.007244	0.010604	LD
				229H2	-	-	-	-	-	
C113	326.97	0.30	0.60	233H1	0.15	0.000370	0.002467	0.007391	0.009858	LD
				233H2	-	-	-	-	-	
C202	366.22	0.30	0.60	275H1	-	-	-	-	-	LD
				275H2	0.15	0.000086	0.000573	0.007593	0.008166	
C203	74.62 (T)	0.25	0.50	267H1	0.25	0.002603	0.010412	0.002942	0.013354	LD
				267H2	0.25	0.002425	0.009700	0.002942	0.012642	
C204	560.89	0.70	0.40	251H1	0.20	0.000504	0.002520	0.005323	0.007843	LD
				251H2	0.20	0.001928	0.009640	0.005323	0.014963	
C205	43.53	0.60	0.40	255H1	0.20	0.002636	0.013180	0.004354	0.017534	LD
				255H2	0.20	0.003489	0.017445	0.004354	0.021799	
C206	76.31	0.60	0.40	259H1	0.20	0.003264	0.016320	0.004307	0.020627	LD
				259H2	0.20	0.003618	0.018090	0.004307	0.022397	
C207	558.21	0.70	0.40	263H1	-	-	-	-	-	LD
				263H2	0.20	0.000777	0.003885	0.005334	0.009219	
C208	558.36	0.30	0.60	238H1	0.15	0.000002	0.000014	0.008392	0.008406	LD
				238H2	0.15	0.000262	0.001747	0.008392	0.010139	
C209	403.17	0.30	0.60	242H1	0.30	0.000006	0.000020	0.003497	0.003517	LD
				242H2	0.30	0.000732	0.002440	0.003497	0.005937	
C210	509.00	0.30	0.60	247H1	-	-	-	-	-	LD
				247H2	0.15	0.000215	0.001433	0.008138	0.009571	

Table 6 contd. Performance level of columns.

Member	P (kN)	B (m)	H (m)	Hinge No	L_p (m)	θ_p (rad)	ϕ_p	ϕ_y	ϕ_{tot}	Result
C302	155.33	0.30	0.60	276H1	-	-	-	-	-	LD
				276H2	0.15	0.001248	0.008320	0.006641	0.014961	
C303	48.62 (T)	0.25	0.50	268H1	0.25	0.001958	0.007832	0.003053	0.010885	LD
				268H2	0.25	0.002389	0.009556	0.003053	0.012609	
C304	272.12	0.70	0.40	252H1	0.20	0.002105	0.010525	0.004728	0.015253	LD
				252H2	0.20	0.003594	0.017970	0.004728	0.022698	
C305	22.89	0.60	0.40	256H1	0.20	0.003827	0.019135	0.004306	0.023441	LD
				256H2	0.20	0.005194	0.025970	0.004306	0.030276	
C306	38.52	0.60	0.40	260H1	0.20	0.003404	0.017020	0.004181	0.021201	LD
				260H2	0.20	0.004685	0.023425	0.004181	0.027606	
C307	288.91	0.70	0.40	264H1	0.20	0.001154	0.005770	0.004774	0.010544	LD
				264H2	0.20	0.002676	0.013380	0.004774	0.018154	
C308	291.96	0.30	0.60	239H1	0.30	0.000256	0.000853	0.003225	0.004078	LD
				239H2	0.30	0.002950	0.009833	0.003225	0.013058	
C309	179.03	0.30	0.60	243H1	0.30	0.000469	0.001563	0.002992	0.004555	LD
				243H2	0.30	0.002586	0.008620	0.002992	0.011612	
C310	266.88	0.30	0.60	248H1	0.15	0.000088	0.000587	0.006918	0.007505	LD
				248H2	0.15	0.000918	0.006120	0.006918	0.013038	

6. Conclusions

A school building was totally collapsed during the 2011 Van earthquake. In this paper, a numerical model was created considering projects and in-situ investigations made after earthquake. In accordance with Turkish Seismic Code (TSC, 2007), pushover analyses were performed and expected member by member damage levels and overall structural damage were determined. According to numerical results, the expected member damage levels of columns, beam and shear walls are less than or equal to the moderate damage level given in the code. Additionally, the expected overall structural earthquake performance according to Turkish Seismic Code (TSC, 2007) is life safety. These numerical results are completely different from the actual case. The analyses carried out in this study, clearly showed that the school building would not have partially collapsed, if it had been properly constructed as planned during design phase. As explained in detail above, the violation of reinforcement detailing rules as well as use of poor quality of concrete seem to be the main reason of actual damage. It should be noted that available earthquake performance assessment methodologies do not consider this type of local deficiencies that can cause partial or total collapse. In order to prevent similar potential future catastrophic consequences, it is strongly recommended that local problems should be taken into consideration in the seismic performance assessment procedures. For doing that, more information is needed on the behavior of substandard existing structural members and their connections which fail through various mechanisms due to poor reinforcement detailing and low-quality concrete. Since there are only limited studies on this type of behavior, the inclusion of effects of these local deficiencies on structural modelling is not taken into the scope of the current study.

Acknowledgements

Our sincere appreciations and gratitude go to our colleagues Nilgün Merve ÇAĞLAR and Alper İLKİ for their supports during the construction of this study.

References

AFAD (n.d.). Turkish Prime Ministry Disaster and Emergency Management Presidency. Retrieved from http://www.afad.gov.tr

Bedirhanoglu I, Ilki A, Pujol S, Kumbasar N (2010). Behavior of deficient joints with plain bars and low-strength concrete. *ACI Structural Journal*, 107(3), 300–310.

Carvalho G, Bento R, Bhatt C (2013). Nonlinear static and dynamic analyses of reinforced concrete buildings – comparison of different modelling approaches. *Earthquakes and Structures, An Int'l Journal*, 4(5), 451–470.

Cosgun C, Dindar AA, Seckin E, Onen Y (2013). Analysis of building damage caused by earthquake in Eastern Turkey. *Gradevinar*, 65(8), 743–752.

CSI (2016). SAP2000. Analysis Reference Manual. CSI: Berkeley (CA, USA): Computers and Structures INC.

Ilki A, Demir C, Bedirhanoglu I, Kumbasar N (2009). Seismic retrofit of brittle and low strength RC columns using fiber reinforced polymer

and cementitious composites. *Advances in Structural Engineering*, 12(3), 325–347.

IMBSEN software systems (2004). XTRACT V3.0.1.: Cross sectional structural analysis of components.

Inel M, Meral E (2016). Seismic performance of RC buildings subjected to past earthquakes in Turkey. *Eartquakes and Structures, An Int'l Journal*, 11(3), 483–503.

Isik E, Kutanis M (2015). Performance based assessment for existing residential buildings in Lake Van basin and seismicity of the region. *Earthquakes and Structures, An Int'l Journal*, 9(4), 893–910.

Mander JB, Priestley MJN, Park R (1988). Observed stress-strain behavior of confined concrete. *Journal of Structural Engineering*, 114(8), 1827–1849.

Ni P (2014). Seismic assessment and retrofitting of existing structure based on nonlinear static analysis. *Structural Engineering and Mechanics*, 49(5), 631–644.

Palermo P, Hernandez RR, Mazzoni S, Trombetti T (2014). On the seismic behavior of a reinforced concrete building with masonry infills collapsed during the 2009 L'Aquila earthquake. *Earthquakes and Structures, An Int'l Journal*, 6(1), 45–69.

Tapan M, Comert M, Demir C, Sayan Y, Orakcal K, Ilki A (2013). Failures of structures during the October 23, 2011 Tabanlı (Van) and November 9, 2011 Edremit (Van) earthquakes in Turkey. *Engineering Failure Analysis*, 34, 606–628.

TSC (2007). Turkish Earthquake Resistant Design Code (TSC). Ministry of Public Works and Settlement. Ankara.

Turk M, Comert M, Cosgun C (2013). Seismic upgrade of RC buildings using CFRP sheets. *Gradevinar*, 65(5), 435–448.

Yön B, Sayın E, Köksal TS (2013). Seismic response of buildings during the May 19, 2011 Simav, Turkey earthquake. *Earthquakes and Structures, An Int'l Journal*, 5(3), 343–357.